

Mechanisms and Molecular Targets of BuShenHuoXue Formula for Osteoarthritis

Wen Xiong,[∇] Jiazheng Zhao,[∇] Xiaowei Ma, and Zhangying Feng*Cite This: *ACS Omega* 2022, 7, 4703–4713

Read Online

ACCESS |



Metrics & More

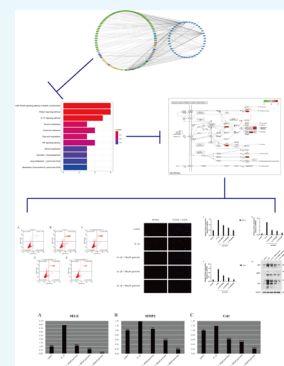


Article Recommendations



Supporting Information

ABSTRACT: The aim was to identify latent mechanism of BuShenHuoXue (BSHX) formula for the management of osteoarthritis (OA) through the network pharmacology approach and experimental validation. We obtained OA-related targets through the Gene Expression Omnibus database and bioactive ingredients with corresponding targets in the formula via the Traditional Chinese Medicine Systems Pharmacology database. Subsequently, networks of the protein–protein interaction and compound–disease target were created and enrichment analysis was implemented. Furthermore, *in vitro*, IL-1 β was applied to rat chondrocytes to mediate apoptosis through inflammation and the Alcian blue and type II collagen staining was used to observe cell morphology. The TUNEL and DAPI staining was performed to observe chondrocyte apoptosis, and the apoptosis rates were gauged via flow cytometry. In addition, we utilized Western blot and PCR to detect the protein and mRNA expression, respectively. A total of 104 potential chemicals and 42 intersecting targets were screened out. Quercetin and luteolin from BSHX formula were principal ingredients. The experiment validated quercetin might suppress chondrocyte apoptosis mediated by IL-1 β and reduce SELE, MMP2, and COL1 expression. Via the AGE-RAGE signaling pathway in diabetic complications, quercetin could aim at SELE, MMP2, and COL1 and exert antagonistic effects against OA.



1. INTRODUCTION

Osteoarthritis (OA) is a frequent ailment that occurs in all joints of the body, such as the hip, knee, shoulder, spine, etc. Research shows that OA afflicts more than 360 million people worldwide,¹ and its morbidity incidence is increasing year by year.² A total of 80 percent of the patients present exercise limitations and 25 percent have physical disability.³ Although scholars have conducted numerous studies of OA, the pathogenesis of OA has been exactly unclear.⁴ So far, the pharmacological management of OA has targeted the symptoms, rather than the underlying etiological factors such as SELE, MMP2, and COL1 that have been recognized as acting essential factors in the inflammatory response of OA.^{5–7} Given the high morbidity rate of OA and the shortage of long-term effective pharmacological therapies, it is imperative to discover potential chemicals with ameliorative effects.

Traditional Chinese Medicine (TCM) dates back from ancient China and has provided substantial advances in the medical field.^{8,9} With minimal side effects, it shows better prospect as complementary or alternative medicine for OA. Furthermore, it shows remarkable effects in protecting articular cartilage.^{10,11} In TCM philosophy, continuous homeostatic preservation and regeneration of cartilage and bone depend on adequate liver and kidney essence.¹² The BuShenHuoXue (BSHX) formula, which consist of 10 main herbs (*Carthamus tinctorius*, *Glycyrrhiza uralensis*, *Rehmannia glutinosa*, *Eucommia ulmoides*, *Prunus persica*, *Lycium barbarum*, *Cinnamomum cassia*, *Cornus officinalis*, *Aconitum carmichaeli*, *Dioscoreae opposita*), has been applied in the management of OA over several years with

promising results.^{13,14} Since the uncertainty in the mechanism of action of herbal medicines can greatly affect their clinical application, the specific therapeutic function of BSHX on OA needs to be urgently defined.

In the present study, we obtained OA-associated targets via the Gene Expression Omnibus (GEO) database and bioactive ingredients with corresponding targets in the formula via the Traditional Chinese Medicine Systems Pharmacology (TCMSP) database. Furthermore, networks of the protein–protein interaction and compound–disease target were created and enrichment analysis was implemented. A series of subsequent experiments were performed, which validated the therapeutic role of bioactive ingredients for BSHX on OA.

2. RESULTS

2.1. Bioactive Chemicals with Their Targets in BuShenHuoXue. Total 1408 chemicals and 10,987 targets of BSHX were obtained through the TCMSP database. After filtering based on oral bioavailability (OB) and drug-likeness, we obtained 269 bioactive chemicals and 3591 targets in all. The

Received: December 24, 2021

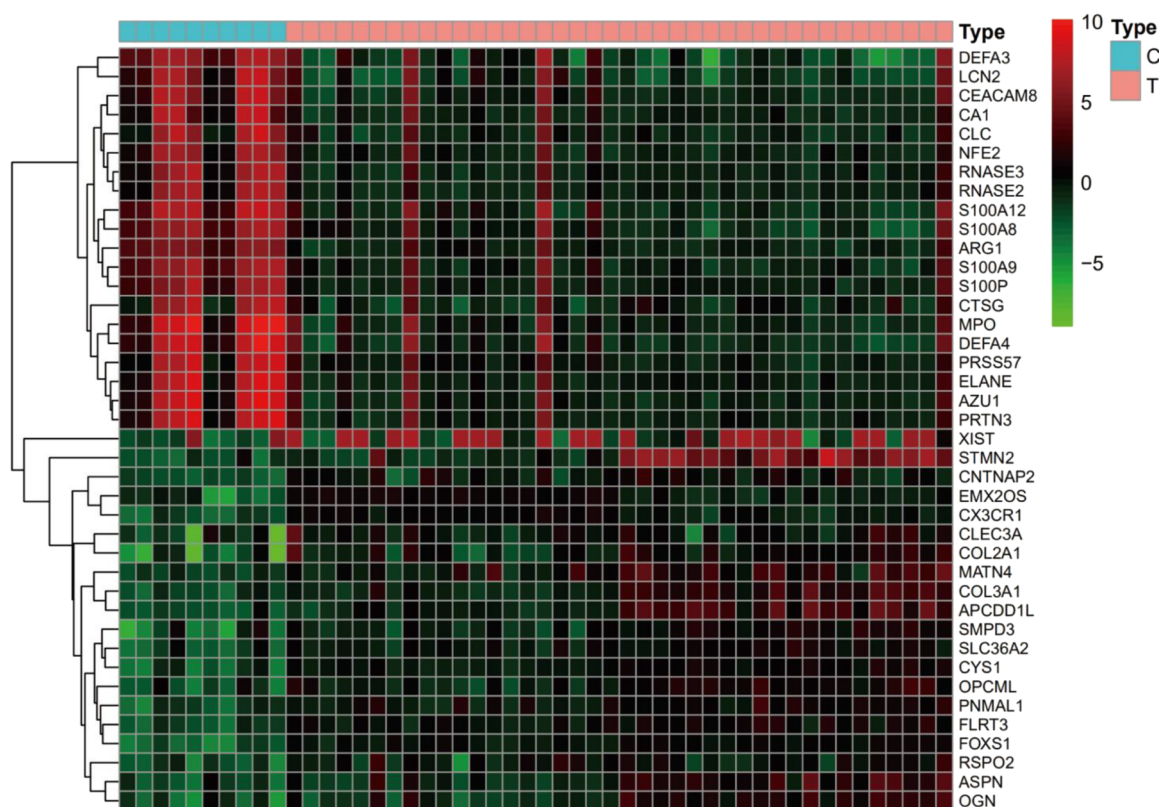
Accepted: January 19, 2022

Published: January 27, 2022



Table 1. The Screening Result of Bioactive Chemicals and Targets in BSHX Formula

	total ingredients	ingredients after screening by OB \geq 30%	ingredients after screening by DL \geq 0.18	total targets	targets after screening
Duzhong	147	66	28	1487	532
Fuzi	65	28	21	139	30
Gancao	280	143	92	2506	1769
Gouqizi	188	91	45	1202	364
Honghua	189	70	22	1466	449
Shanyao	71	41	16	851	144
Shanzhuyu	226	102	20	1843	130
Shudihuang	76	25	2	327	34
Taoren	66	30	23	342	139
Rougui	100	50	0	824	0
total	1408	646	269	10,987	3591

**Figure 1.** Top 40 DEGs between normal tissues and OA tissues.

results of 269 chemicals and screening parameters of BSHX are presented in Table 1.

2.2. OA-Related Targets. The GSE51588 dataset contains 50 samples, including 40 experimental samples (OA) and 10 control samples (normal), from which we acquired a total of 21,752 targets associated with OA. By differential analysis, 1591 differentially expressed genes (DEGs) were obtained, of which 641 were down-regulated and 950 were up-regulated. The heat map shows top 40 DEGs (Figure 1).

2.3. Compound-Disease Target Network Construction. After intersection of 1591 DEGs in OA with the BSHX target, 42 genes were identified. Incorporating 104 corresponding bioactive chemicals, a compound-disease target network consisting of 146 nodes and 208 edges (Figure 2) was constructed. Every compound was associated with at least one gene, and chemicals possessing the most OA targets were quercetin (MOL000098) possessing 22 edges and luteolin (MOL000006) possessing 9 edges, indicating that these

chemicals might be bioactive ingredients for BSHX in the management of OA.

2.4. Construction of the Protein–Protein Interaction (PPI) Network. The PPI network displayed interactions of the compound-disease target in OA. The general network contained 1229 nodes and 15,419 edges. By using topological analysis for screening, we initially obtained the network possessing 124 nodes and 2358 edges and finally identified the kernel network possessing 31 nodes and 287 edges (Figure 3).

2.5. Gene Ontology (GO) and Kyoto Encyclopedia of Genes and Genomes (KEGG) Enrichment Analyses. Figure 4 demonstrates the outcome of target protein GO analysis. The entry with the most significant enrichment is extracellular structure organization. Figure 5 and Table 2 demonstrate the outcome of KEGG analysis. The major pathways for herbal intervention in OA are the AGE-RAGE signaling pathway in diabetic complications (hsa04933), relaxin signaling pathway (hsa04926), IL-17 signaling pathway (hsa04657), tyrosine

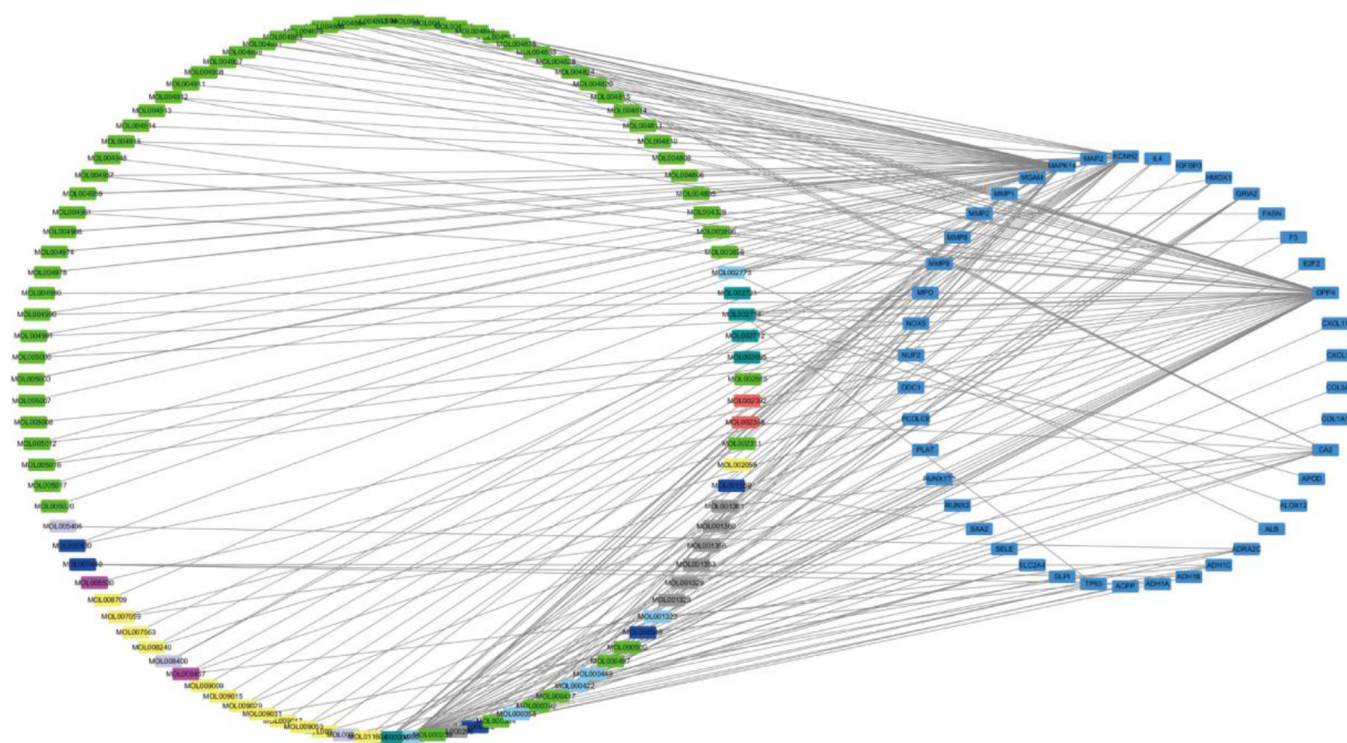


Figure 2. Network of 104 bioactive chemicals and 42 interacting targets of BSHX and OA.

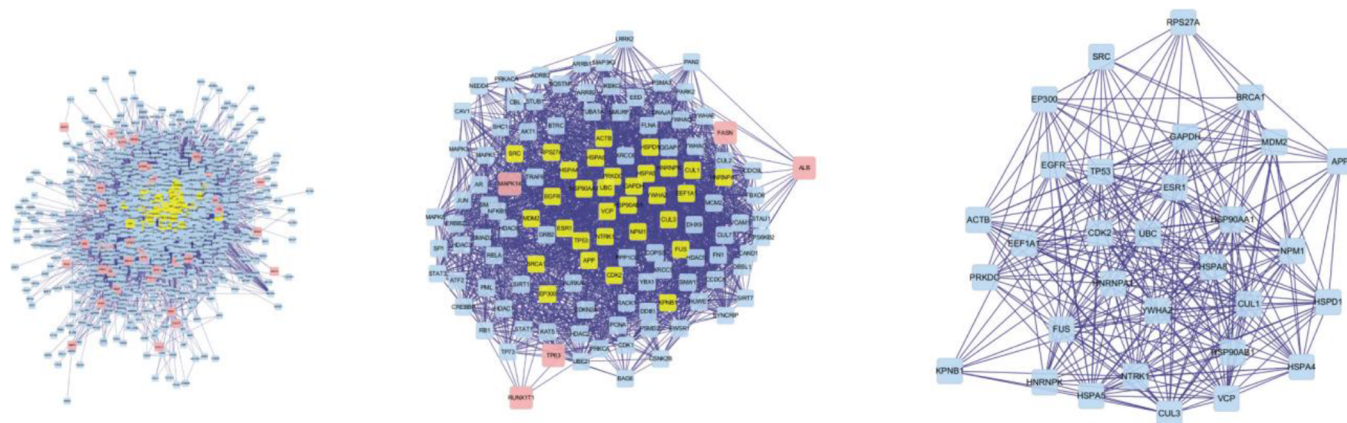


Figure 3. PPI network of interacting genes of BSHX against OA.

metabolism (hsa00350), and endocrine resistance (hsa01522). Typically, Figure 6 displays the location of BSHX targets including SELE, MMP2, and COL1.

2.6. Observation of the Culture Results of Rat Chondrocytes. After digestion and isolation of primary cells, 80–90% of the cells were fused after 10–14 days of culture. The Alcian blue staining (Figure 7A) and type II collagen staining (Figure 7B) was used to observe cell morphology.

2.7. Quercetin Suppressed the Chondrocyte Apoptosis. The results were observed by flow cytometry where the chondrocyte apoptosis rate in the control group was 1.73% (Figure 8A), and the experimental group (IL-1 β group, IL-1 β + 100 μ M quercetin group, IL-1 β + 200 μ M quercetin group, and IL-1 β + 400 μ M quercetin group) of chondrocyte apoptosis has rates of 12.09 (Figure 8B), 8.78% (Figure 8C), 6.31 (Figure 8D), and 4.31% (Figure 8E).

The TUNEL and DAPI staining (Figure 9) was used to observe the apoptosis of chondrocytes under a fluorescence

microscope, which could be further verified more intuitively, indicating that versus the control group, IL-1 β can remarkably enhance chondrocyte apoptosis, while quercetin can effectively reduce the apoptosis induced by IL-1 β .

2.8. Quercetin Decreased the mRNA Expression of SELE, MMP2, and COL1. PCR result revealed the mRNA expression levels of SELE, MMP2, and COL1. By taking actin as the internal reference, we set the relative expression rate of actin as 1 and obtained the relative expression rates of the three genes in each group. The mRNA expression levels of SELE (Figure 10A), MMP2 (Figure 10B), and COL1 (Figure 10C) were significantly increased due to the inflammatory mediating effect of IL-1 β , which could also be gradually decreased with the addition of quercetin dose.

2.9. Quercetin Decreased the Protein Expression of SELE, MMP2, and COL1. Through the Western blotting result, the change in trends of SELE, MMP2, and COL1 expression were similar to those in PCR. Using GAPDH as the internal

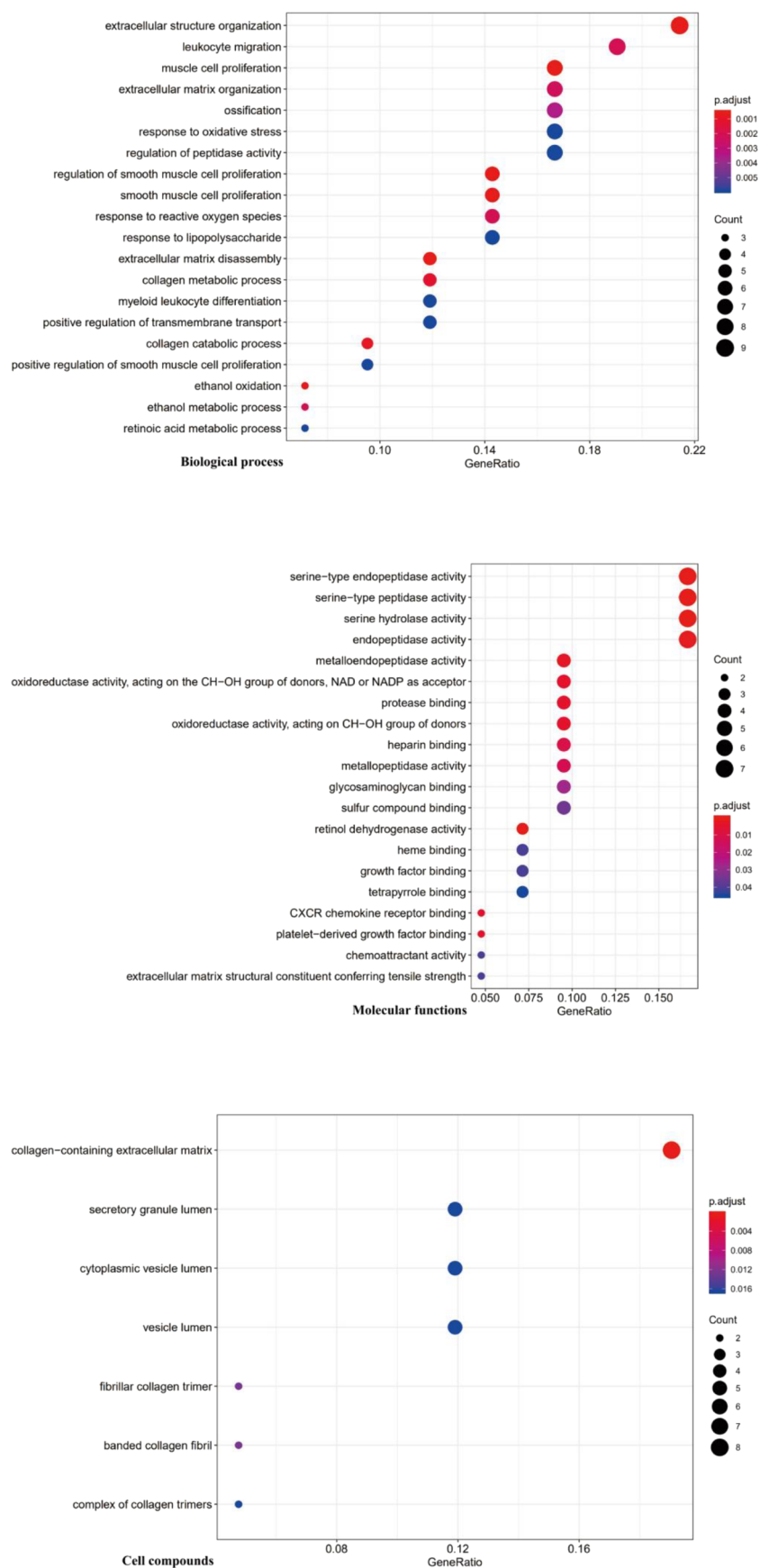


Figure 4. GO enrichment analysis.

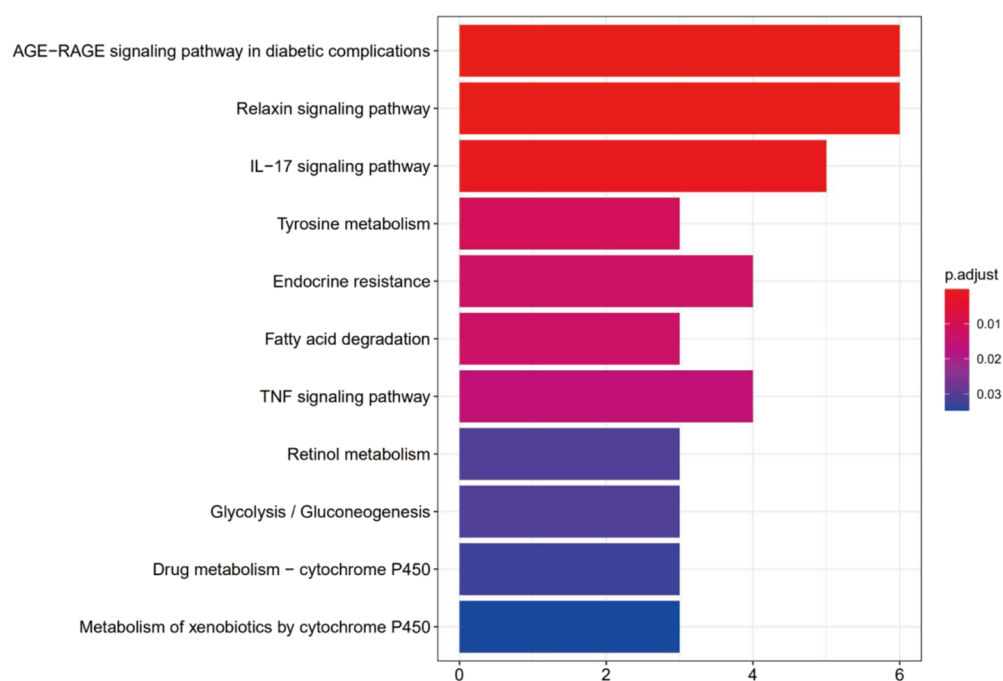


Figure 5. Enriched KEGG pathways.

Table 2. KEGG Enrichment Analysis

ID	description	adj. P value	q value	gene ID
hsa04933	AGE-RAGE signaling pathway in diabetic complications	<0.001	<0.001	SELE/MAPK14/MMP2/F3/COL1A1/COL3A1
hsa04926	relaxin signaling pathway	<0.001	<0.001	MMP1/MAPK14/MMP2/MMP9/COL1A1/COL3A1
hsa04657	IL-17 signaling pathway	0.001	0.001	MMP1/MAPK14/MMP9/CXCL10/IL4
hsa00350	tyrosine metabolism	0.011	0.009	ADH1C/ADH1B/ADH1A
hsa01522	endocrine resistance	0.013	0.011	MAPK14/MMP2/MMP9/E2F2
hsa00071	fatty acid degradation	0.013	0.011	ADH1C/ADH1B/ADH1A
hsa04668	TNF signaling pathway	0.016	0.014	SELE/MAPK14/MMP9/CXCL10
hsa00830	retinol metabolism	0.031	0.026	ADH1C/ADH1B/ADH1A
hsa00010	glycolysis/gluconeogenesis	0.031	0.026	ADH1C/ADH1B/ADH1A
hsa00982	drug metabolism, cytochrome P450	0.033	0.028	ADH1C/ADH1B/ADH1A
hsa00980	metabolism of xenobiotics by cytochrome P450	0.035	0.030	ADH1C/ADH1B/ADH1A

reference, we obtained relative expression rates of three proteins. Western blot revealed that quercetin antagonized the inflammatory-inducing effect of IL-1 β , and protein expression of SELE, MMP2, and COL1 was remarkably reduced in the added quercetin group, with the most pronounced inflammatory antagonistic effect of 400 μ M quercetin (Figure 11A–D).

3. DISCUSSION

The etiology of OA is still unclear. As a prevalent disease, it is characterized by degenerative changes in articular cartilage, with synovitis as the main manifestation.^{15–19} Owing to the increase in associated risk factors, there is a growing concern about the disease regression and life quality of OA patients and an urgent need for emerging OA treatment strategies.²⁰

OA was first recorded in the book "Huangdi Neijing" in which the etiology and pathogenesis were described in detail. The basic pathogenesis of OA is local qi stagnation and blood stasis in the theory of TCM. TCM chemicals regulate the progression of OA by interfering with some targets in a certain signaling pathway.²¹ Currently, the main etiological treatment is kidney tonifying and blood activating.

TCM acts as a promising therapeutic choice for OA. The BSHX formula is a traditional Chinese remedy that proved to be efficient for quite a long time in China. Prior research studies have shown that the BSHX formula might prohibit the degradation of articular cartilage in vivo. It was found that after 8 weeks of treatment with kidney-tonifying and blood-activating prescription, IL-6 and MMP-13 in knee joint fluid of rabbits with knee arthritis were reduced. Their study uncovered that the BSHX formula attenuated osteoarthritic cartilage degradation as the herbal MMP13 suppressor via the TGF- β /MMP13 signaling pathway.¹³

From the system biology perspective, the network pharmacology (NP) method has been advocated to reinforce the established methodology for pharmacology.^{22–25} Zhu et al. undertook a predictive analysis of the action of Shaoyao Gancao Decoction (SGD) in OA through the NP method, and the results suggested that SGD may function as a pharmacological agent in OA through various pathways such as immunomodulation, apoptosis, and cell cycle.²¹ Zhang et al. used an NP method to clarify the possible potential mechanisms of Radix Achyranthis Bidentatae (RAB) for the management of OA.²⁶ Results showed that RAB may regulate disease onset and progression by defending the synovial membrane and cartilage

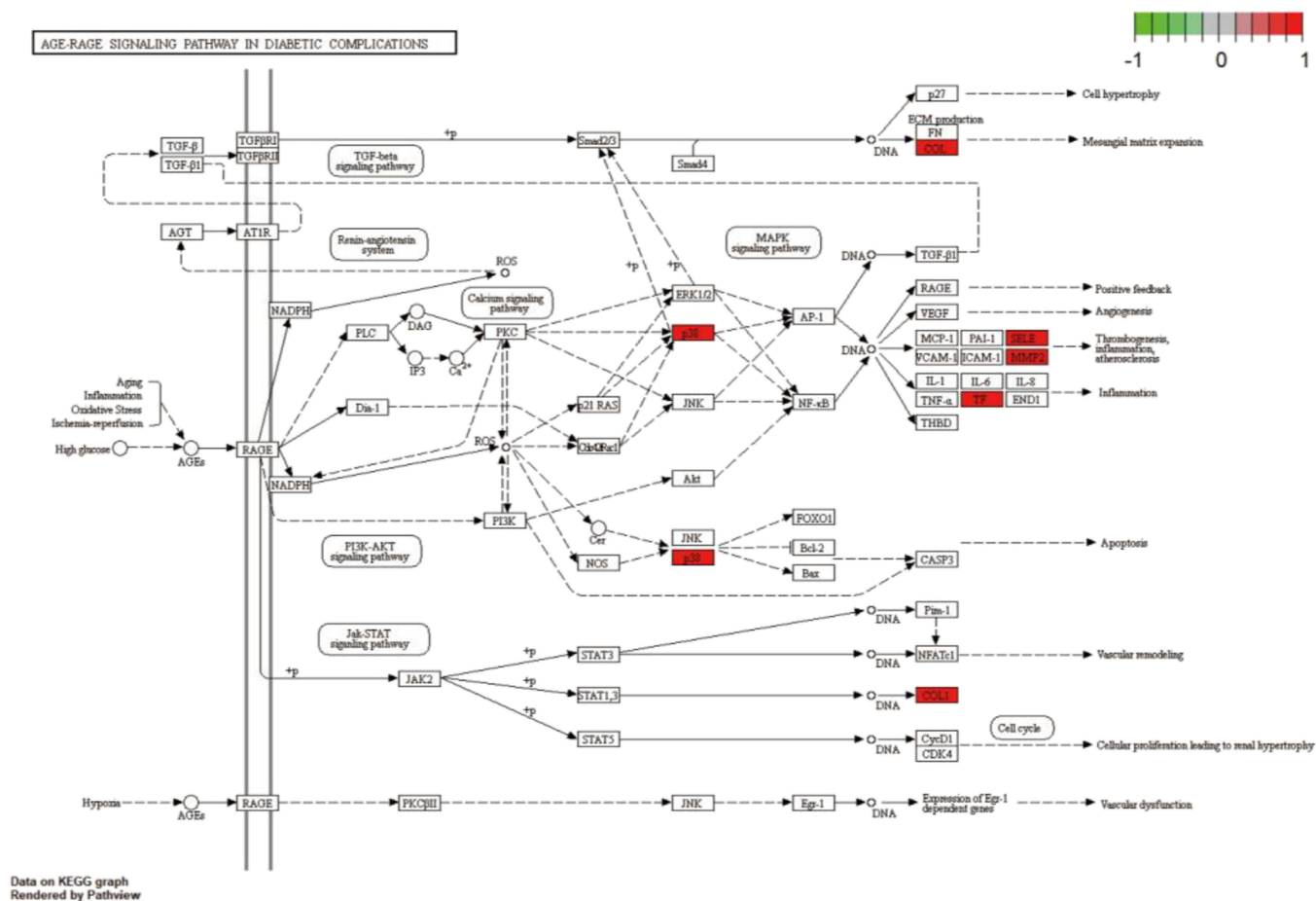


Figure 6. Distribution of BSHX targets (red nodes).

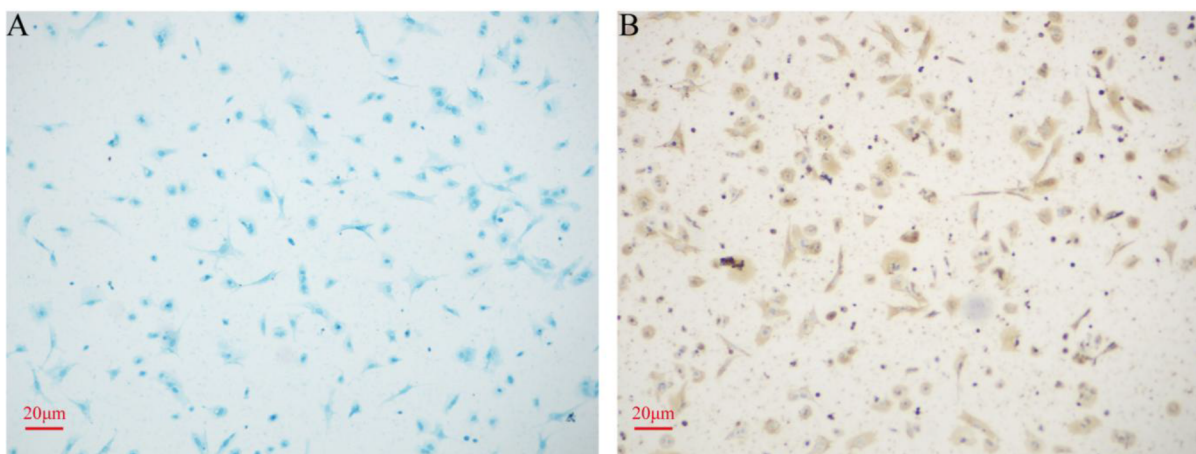


Figure 7. Chondrocyte morphology observation. (A) Alcian blue staining (×200). (B) Type II collagen staining (×200).

as well as modulating inflammatory and immune responses.²⁶ However, no further research was conducted to verify the prediction in both two research studies, thus reducing their persuasiveness and credibility.

In our study, 104 chemicals and 42 target genes were identified, and every compound was associated with at least one DEG in OA. A great majority of chemicals were derived from licorice, suggesting that licorice may be the principal efficacious herb of BSHX in the management of OA, and other herbs could play supporting roles. Quercetin and luteolin are bioactive components possessing most targets and exist in herbal

compounds (quercetin from licorice, Lycii Fructus, Carthami Flos, and Eucommiae Cortex; luteolin from Carthami Flos).

OA is featured by the unusual extracellular matrix content (ECM) combined with articular surface erosion.²⁷ The precisely regulated homeostasis of ECM synthesis, metabolism, and repairment is impaired, leading to the gradual degradation of the articular cartilage. Enrichment analysis of the biological process (BP) revealed that potential functions of these chemicals against OA are extracellular structure organization, muscle cell proliferation, and extracellular matrix disassembly. The most significant potential pathway is the AGE-RAGE signaling

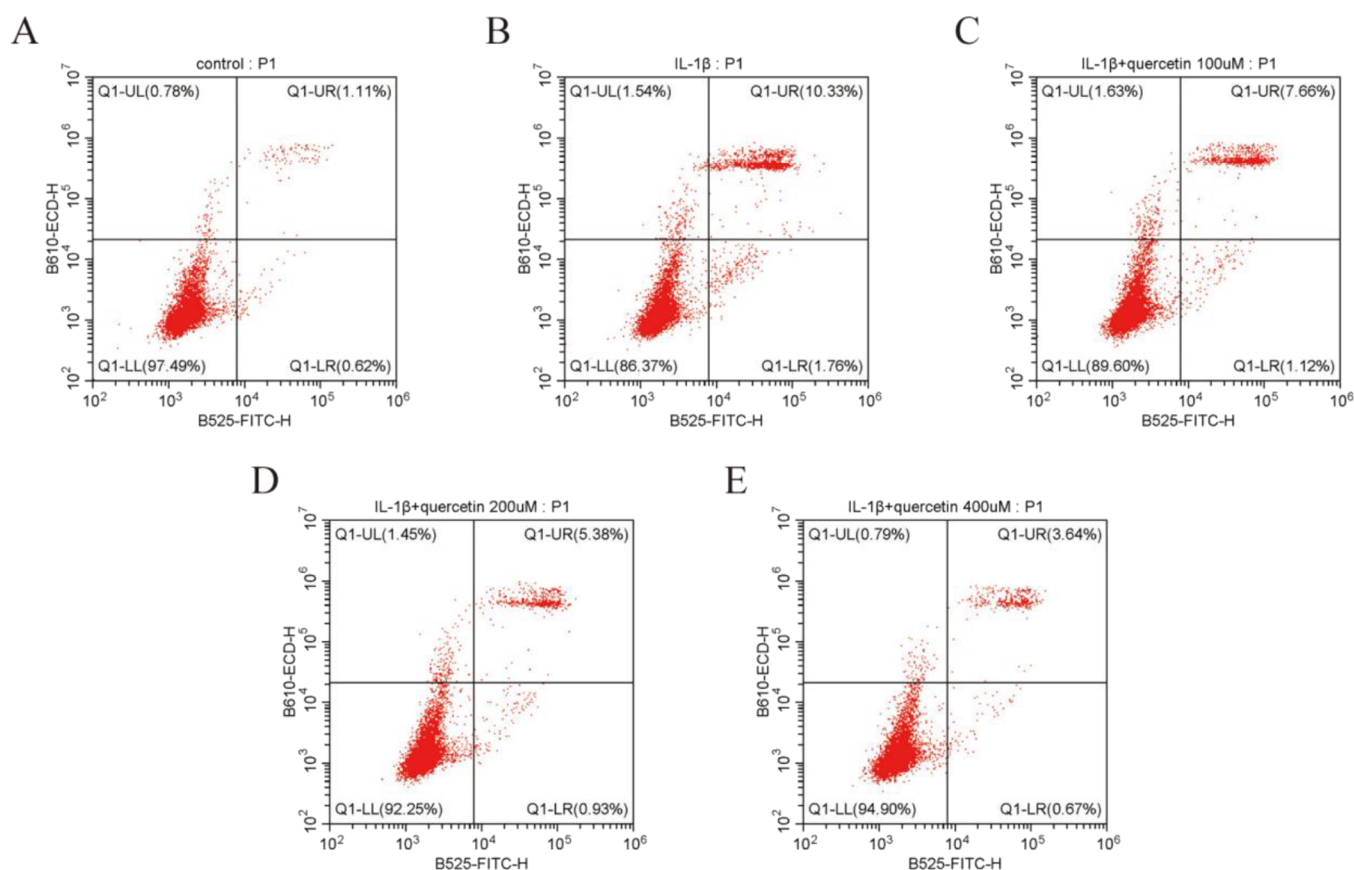


Figure 8. Flow cytometry analysis of apoptosis in chondrocytes. (A) Control group. (B) IL-1 β group. (C) IL-1 β + 100 μ M quercetin group. (D) IL-1 β + 200 μ M quercetin group. (E) IL-1 β + 400 μ M quercetin group.

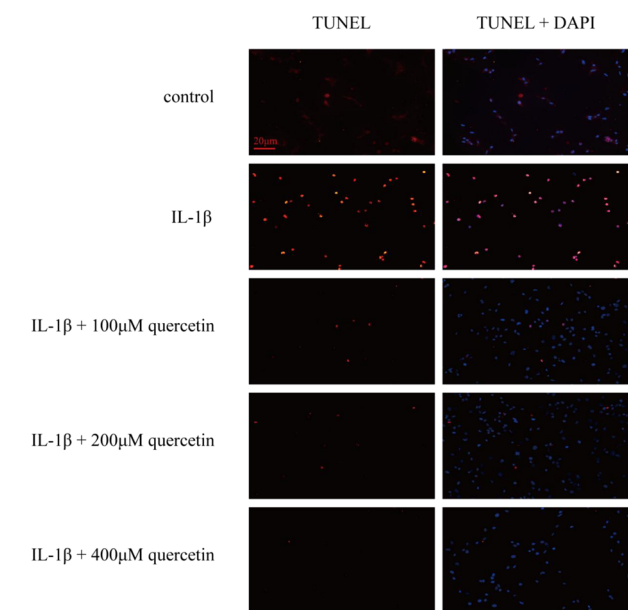


Figure 9. TUNEL and DAPI staining in five groups of chondrocytes ($\times 200$).

pathway in diabetic complications. It is noteworthy that among the three target genes (SELE/ MMP2/COL1) in this pathway, all of them can be interfered by quercetin in our validation experiments, suggesting that quercetin may be the most promising compound for OA therapy in BSHX. Quercetin was reported to exhibit analgesic effects in various pain models and,

specially, can relieve CAR-mediated hyperalgesia,²⁸ chemotherapy-mediated neuralgia,²⁹ and diabetic neuralgia.³⁰ Demonstrating the collaborative effect and capacity to oxidative stress as an antioxidant, quercetin has been employed successfully as supplementary in vivo and in experimental arthritic models.^{31,32}

In the present study, we applied an emerging and efficient method for the identification of bioactive ingredients, intersecting targets, and potential mechanisms in the traditional Chinese herbal formula—BSHX formula. Nevertheless, our study has some limitations. First, the omission of synergistic effects among ingredients in herbal formula may cause bias and incomplete results. Furthermore, whether quercetin can also protect cartilage and treat OA in vivo, as well as the evaluation of its effective dose concentration, needs to be further discussed and verified by corresponding experiments.

4. CONCLUSIONS

We applied NP to search out intersecting targets and underlying mechanisms in the BSHX formula for the management of OA and ultimately focused on quercetin as the main biologically active ingredient, which might suppress the osteoarthritic process via the AGE-RAGE signaling pathway in diabetic complications involving SELE, MMP2, and COL1. Further validation experiments confirmed that quercetin could suppress the chondrocyte apoptosis mediated by IL-1 β . By the mechanism of down-regulating SELE, MMP2, and COL1 expression, we made sure that quercetin exerts a protective function on the cartilage. In addition, more research on reducing

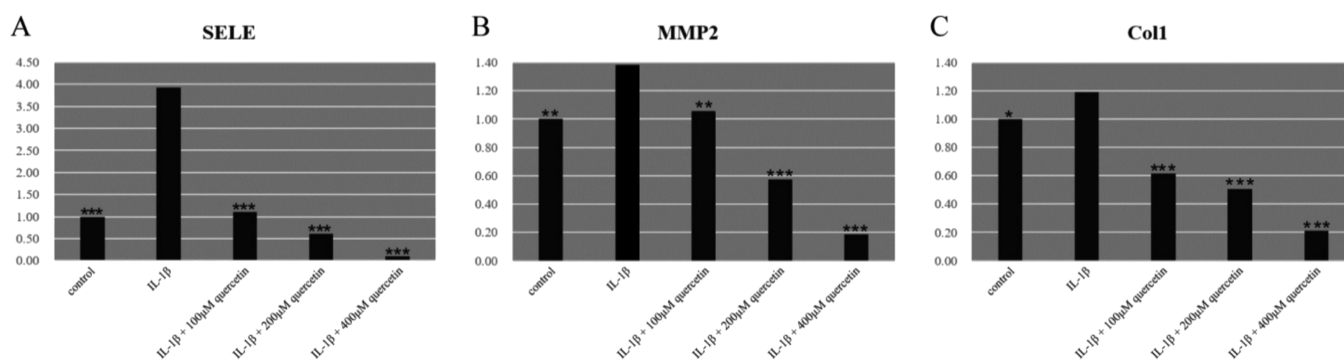


Figure 10. Relative mRNA expression rates of genes in chondrocytes by PCR. (A) SELE. (B) MMP2. (C) COL1. * $P < 0.05$, ** $P < 0.01$, *** $P < 0.001$ versus the IL-1 β group.

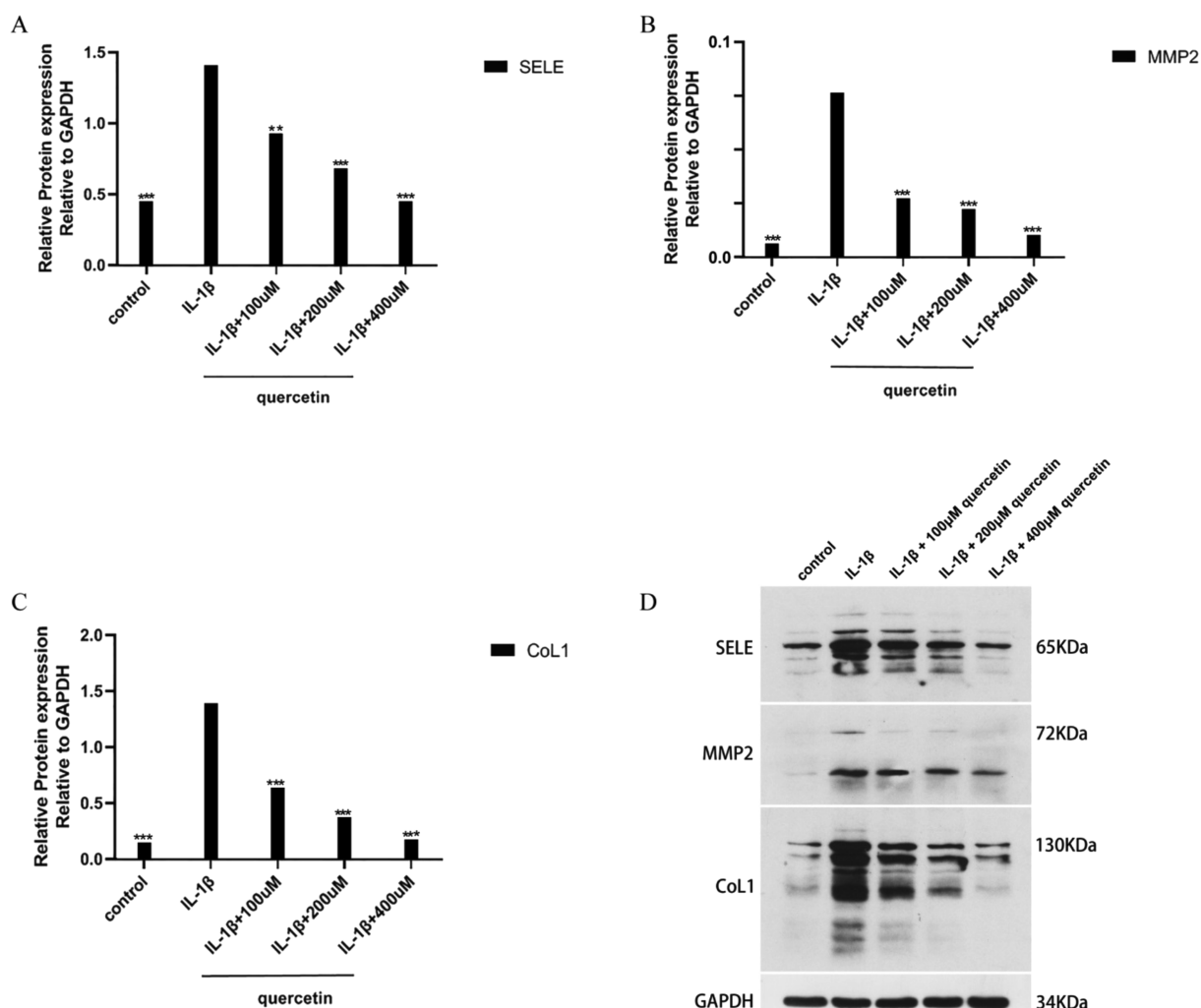


Figure 11. Western blot in five groups of chondrocytes. (A) SELE. (B) MMP2. (C) COL1. (D) Electrophoretic images. ** $P < 0.01$, *** $P < 0.001$ versus IL-1 β group.

the toxicity of TCM and proving the rationality and compatibility is needed.

5. MATERIALS AND METHODS

5.1. Data Mining: Screening out Bioactive Chemicals and Targets in the BSHX Formula. Chemicals and targets of individual herbs (*Aconitum carmichaeli*, *Glycyrrhiza uralensis*, *Lycium barbarum*, *Rehmannia glutinosa*, *Eucommia ulmoides*,

Cinnamomum cassia, *Cornus officinalis*, *Prunus persica*, *Carthamus tinctorius*, *Dioscoreae opposita*) in the BSHX Formula (Table 3) were mined from the TCMSP database (<http://tcmispw.com/tcmisp.php>).³³ The screening criteria of herbs are absorption, distribution, metabolism, and excretion (ADME) including OB, DL, P450, etc.³⁴ OB $\geq 30\%$ and DL ≥ 0.18 are chosen as filtering criteria for underlying bioactive compositions and corresponding targets via Strawberry-perl software (version 5.30.1.1).

Table 3. BSHX Formula Compositions

Chinese name	botanical name	Latin name
Shu Di Huang	<i>Rehmannia glutinosa</i> (Libosch)	Rehmanniae Radix Praeparata
Du Zhong	<i>Eucommia ulmoides</i> (Oliv.)	Eucommiae Cortex
Fu Zi	<i>Aconitum carmichaeli</i> (Debx.)	Aconiti Lateralis Radix Praeparata
Gou Qi Zi	<i>Lycium barbarum</i> (L.)	Lycii Fructus
Rou Gui	<i>Cinnamomum cassia</i> (Presl)	Cinnamomi Cortex
Shan Zhu Yu	<i>Cornus officinalis</i> (Sieb.)	<i>Cornus Officinalis</i> Sieb. Et Zucc.
Tao Ren	<i>Prunus persica</i> (Batsch.)	Persicae Semen
Hong Hua	<i>Carthamus tinctorius</i> (L.)	Carthami Flos
Shan Yao	<i>Dioscorea opposita</i> (Thunb.)	Rhizoma Dioscoreae
Gan Cao	<i>Glycyrrhiza uralensis</i> (Fisch.)	licorice

5.2. Searching and Screening for Potential OA Targets. OA-associated targets were acquired through GSE51588 dataset via the GEO database (<https://www.ncbi.nlm.nih.gov>).³⁵ The GSE51588 dataset contains 50 samples, including 40 experimental samples (OA) and 10 control samples (normal). The series matrix file and corresponding platform file (GPL13497) were downloaded. Depending on two criteria (adj. $P < 0.05$, $\log_2 \text{FC} > 1$), DEGs were excavated via the limma package of R software (version 3.6.2).

5.3. Construction of Networks. By applying Cytoscape software (version 3.7.2), a compound network with reciprocal targets was generated through the interaction of bioactive composition targets with OA targets in BSHX. Afterward, utilizing Cytoscape software, PPI networks were established. Furthermore, utilizing CytoNCA plug-in, two times topological analysis of the PPI network was carried out depending on the filtering criteria BC degree ≥ 100 and DC degree ≥ 61 .

5.4. GO and KEGG Enrichment Analyses. GO enrichment was executed via ClueGO plug-in of Cytoscape and mainly covered three subclasses: BP, cell chemicals (CC), and molecular functions (MF) ($P \leq 0.05$). KEGG enrichment was accomplished via the bioconductor package of R software ($P \leq 0.05$), and a bar chart presented the top corresponding pathways.

5.5. Cell Culture. Primary chondrocytes were obtained from 20 executed 4 week-old SD rats. The raising environment of rats was maintained with 12 h of light/dark alternation; the temperature was preserved at 21–26 °C; and all rats were kept on diet and water ad libitum. In accordance with the approach proposed by American Veterinary Medical Association, rats were euthanized by intraperitoneal injection of pentobarbital sodium at a dose of 120 mg/kg. The cartilage of the knee joint was dissected under aseptic conditions, and the cartilage was separated from the nearby connective tissue and muscle. The obtained cartilage was chopped into miniscule pieces, digested with 0.25% trypsin for 30 min, and incubated with 0.04% collagenase II at 37 °C overnight. A final centrifugation (2000 rpm, 3 min) was performed to acquire chondrocytes. In a 37 °C, 5% CO₂ incubator (Thermo, Waltham, MA, USA), cells were incubated with DMEM (Thermo, Waltham, MA, USA) incorporating 10% FBS and 1% penicillin/streptomycin (Solarbio, Beijing, China). Post incubation for 48 h, the medium was changed and non-adherent cells were excluded. Afterward, the medium was updated every other day. When the percentage of adherent cells was 85–90%,

subculture was carried out. The third–fifth generation was used for subsequent experiments, and the Alcian blue staining and type II collagen staining was used to observe the cell morphology. Based on previous experience, we selected three quercetin concentrations (100, 200, and 400 μM) for our experiments, which might provide the strongest protection to chondrocytes in vitro.³⁶ Cells were randomized into five groups, and various interventions were given depending on the group: control group (no intervention), IL-1 β group (50 ng/mL), and three quercetin groups (IL-1 β + 100 μM , 200 μM , 400 μM quercetin). Briefly, the chondrocytes were incubated for 6 h after the addition of the corresponding interventions in the medium followed by transfer to the normal medium for 24 h continuous incubation for the apoptosis assay, PCR, and Western blot. This research was approved by the Ethics Committee of Animal Center of Fourth Hospital of Hebei Medical University.

5.6. Apoptosis Assay. The apoptosis rates of each group were gauged via flow cytometry. The Annexin V-FITC/PI apoptosis kit (BD, San Diego, USA) was applied depending on the instructions. In brief, chondrocytes were gathered and rinsed twice with PBS. Afterward, chondrocytes were labeled with 500 μL 1 \times binding buffer comprising 10 μL PI and 5 μL Annexin V-FITC for 5 min at dark. Finally, apoptosis rates were gauged via flow cytometer (BD Biosciences, Franklin Lakes, USA). In addition, morphology of cell death was observed by TUNEL (ApopTag Red in Situ Apoptosis Detection Kit, Chemicon International, Temecula, CA). Furthermore, nuclei was counter-stained with 1 $\mu\text{g}/\text{mL}$ DAPI (Beyotime, Shanghai, China) during 3 min and images were captured by a fluorescence microscope (Axiophot, Zeiss).

5.7. Quantitative Real-Time PCR. TRIzol reagent (TAKARA, Japan) was used by the following instructions, and the reverse transcription reaction was carried out depending on the following cycles: 25 °C for 10 min, 50 °C for 30 min, and 85 °C for 5 min. Fluorescent quantitative PCR kit was used and fluorescent PCR was carried out based on the following cycles: 95 °C for 5 min, 95 °C for 10 s, and 60 °C for 30 s, with a total of 40 cycles. In addition, three replicate wells were produced for each specimen and the solubility curve temperature was adjusted to 60–95 °C. The designed primer sequences for PCR are shown in Table 4.

Table 4. PCR Primer Sequences

gene	primer sequence (5' to 3')
Rat-Actin-F	CTGTGTGGATTGGTGGCTCT
Rat-Actin-R	CAGCTCAGTAACAGTCCGCC
Rat-SELE-F	GTGAAAGGGGGCTATGTGC
Rat-SELE-R	GGCAGGTTGGGTCAAAG
Rat-MMP2-F	CTTCCAGGGCACCTCTTAC
Rat-MMP2-R	ACACATGGGGCACCTTC
Rat-Col1-F	GATGGACTCAACGGTCTCCC
Rat-Col1-R	CGGCCACCATCTTGAGACTT

5.8. Western Blot. Cellular proteins were absorbed via RIPA (Beyotime, Jiangsu, China), and protein concentration was determined by BCA. Protein lysates were electrophoresed in 10% SDS-PAGE at 90 V and transferred to nitrocellulose paper (Millipore, USA) for 2 h at 200 mA. The nitrocellulose paper was blocked with 5% non-fat milk for 1 h at room temperature and then washed three times with TBST. Membranes were incubated with primary antibodies overnight at 4 °C. After three washes with TBST, nitrocellulose paper was probed with HRP

conjugated secondary antibodies for 2 h at room temperature. Eventually, immunoreactive bands were measured with the enhanced chemiluminescence system (Millipore, USA) and results were analyzed using the Quantity One (Bio-Rad, USA). The following antibodies and corresponding dilution ratios were used: anti-SELE (bs-1273R, Rabbit, Bioss, 1:500, secondary antibody: 1:5000), anti-MMP2 (bs-0412R, Rabbit, Bioss, 1:500, secondary antibody: 1:5000), anti-CoL1 (bs-10423R, Rabbit, Bioss, 1:500, secondary antibody: 1:5000), and anti-GAPDH (60004-1-Ig, Mouse, Proteintech, 120,000, secondary antibody, 1:5000).

5.9. Statistical Analysis. Statistical analysis was carried out via the SPSS software (version 21.0). The normally distributed data were analyzed with the *t* test, and the nonparametric variables were analyzed by the Mann–Whitney U test. *P* < 0.05 was considered statistically significant.

■ ASSOCIATED CONTENT

SI Supporting Information

The Supporting Information is available free of charge at <https://pubs.acs.org/doi/10.1021/acsomega.1c07270>.

Amplification curves for PCR (Figure S1) and dissolution curves for PCR (Figure S2) (PDF)

■ AUTHOR INFORMATION

Corresponding Author

Zhangying Feng – Department of Clinical Pharmacology, The Fourth Hospital of Hebei Medical University, Shijiazhuang, Hebei 050011, China; orcid.org/0000-0003-3761-3559; Email: zhangyingfeng0311@163.com

Authors

Wen Xiong – Department of Orthopedics, Wuhan Fourth Hospital; Puai Hospital, Tongji Medical College, Huazhong University of Science and Technology, Wuhan, Hubei 430033, China

Jiazheng Zhao – Department of Orthopedics, The Fourth Hospital of Hebei Medical University, Shijiazhuang, Hebei 050011, China

Xiaowei Ma – Department of Orthopedics, The Fourth Hospital of Hebei Medical University, Shijiazhuang, Hebei 050011, China

Complete contact information is available at: <https://pubs.acs.org/doi/10.1021/acsomega.1c07270>

Author Contributions

[†]W.X. and J.Z.Z. contributed equally to this work.

Notes

The authors declare no competing financial interest.

■ ACKNOWLEDGMENTS

Not Applicable.

■ REFERENCES

- (1) Gu, Y. T.; Chen, J.; Meng, Z. L.; Ge, W. Y.; Bian, Y. Y.; Cheng, S. W.; Xing, C. K.; Yao, J. L.; Fu, J.; Peng, L. Research progress on osteoarthritis treatment mechanisms. *Biomed. Pharmacother.* **2017**, *93*, 1246–1252.
- (2) Thomas, A. C.; Hubbard-Turner, T.; Wikstrom, E. A.; Palmieri-Smith, R. M. Epidemiology of Posttraumatic Osteoarthritis. *J Athl Train* **2017**, *52*, 491–496.

- (3) Li, M. H.; Xiao, R.; Li, J. B.; Zhu, Q. Regenerative approaches for cartilage repair in the treatment of osteoarthritis. *Osteoarthr. Cartil.* **2017**, *25*, 1577–1587.

- (4) Hermann, W.; Lambova, S.; Muller-Ladner, U. Current Treatment Options for Osteoarthritis. *Curr Rheumatol Rev* **2018**, *14*, 108–116.

- (5) Haltmayer, E.; Ribitsch, I.; Gabner, S.; Rosser, J.; Gueltekin, S.; Peham, J.; Giese, U.; Dolezal, M.; Egerbacher, M.; Jenner, F. Co-culture of osteochondral explants and synovial membrane as in vitro model for osteoarthritis. *PLoS One* **2019**, *14*, No. e0214709.

- (6) Cai, P.; Jiang, T.; Li, B.; Qin, X.; Lu, Z.; Le, Y.; Shen, C.; Yang, Y.; Zheng, L.; Zhao, J. Comparison of rheumatoid arthritis (RA) and osteoarthritis (OA) based on microarray profiles of human joint fibroblast-like synoviocytes. *Cell Biochem. Funct.* **2019**, *37*, 31–41.

- (7) Herr, S. A.; Malek, S.; Rochat, M. C.; Moore, G. E.; Ko, J. C.; Shi, R. Evidence of acrolein in synovial fluid of dogs with osteoarthritis as a potential inflammatory biomarker. *BMC Musculoskelet Disord* **2021**, *22*, 894.

- (8) Tao, W.; Luo, X.; Cui, B.; Liang, D.; Wang, C.; Duan, Y.; Li, X.; Zhou, S.; Zhao, M.; Li, Y.; He, Y.; Wang, S.; Kelley, K. W.; Jiang, P.; Liu, Q. Practice of traditional Chinese medicine for psycho-behavioral intervention improves quality of life in cancer patients: A systematic review and meta-analysis. *Oncotarget* **2015**, *6*, 39725–39739.

- (9) Hao, P.; Jiang, F.; Cheng, J.; Ma, L.; Zhang, Y.; Zhao, Y. Traditional Chinese Medicine for Cardiovascular Disease: Evidence and Potential Mechanisms. *J. Am. Coll. Cardiol.* **2017**, *69*, 2952–2966.

- (10) Zhu, F.; Yin, L.; Ji, L.; Yang, F.; Zhang, G.; Shi, L.; Xu, L. Suppressive effect of Sanmiao formula on experimental gouty arthritis by inhibiting cartilage matrix degradation: An in vivo and in vitro study. *Int. Immunopharmacol.* **2016**, *30*, 36–42.

- (11) Wang, F.; Shi, L.; Zhang, Y.; Wang, K.; Pei, F.; Zhu, H.; Shi, Z.; Tao, T.; Li, Z.; Zeng, P.; Wang, X.; Ji, Q.; Qin, L.; Xue, Q. A Traditional Herbal Formula Xianlinggubao for Pain Control and Function Improvement in Patients with Knee and Hand Osteoarthritis: A Multicenter, Randomized, Open-Label, Controlled Trial. *Evid Based Complement Alternat Med* **2018**, *2018*, 1827528.

- (12) Li, L.; Liu, H.; Shi, W.; Liu, H.; Yang, J.; Xu, D.; Huang, H.; Wu, L. Insights into the Action Mechanisms of Traditional Chinese Medicine in Osteoarthritis. *Evid Based Complement Alternat Med* **2017**, *2017*, 5190986.

- (13) Wang, P. E.; Zhang, L.; Ying, J.; Jin, X.; Luo, C.; Xu, S.; Dong, R.; Xiao, L.; Tong, P.; Jin, H. Bushenhuoxue formula attenuates cartilage degeneration in an osteoarthritic mouse model through TGF- β /MMP13 signaling. *J Transl Med* **2018**, *16*, 72.

- (14) Xu, H. H.; Li, S. M.; Xu, R.; Fang, L.; Xu, H.; Tong, P. J. Predication of the underlying mechanism of Bushenhuoxue formula acting on knee osteoarthritis via network pharmacology-based analyses combined with experimental validation. *J. Ethnopharmacol.* **2020**, *263*, 113217.

- (15) Pottie, P.; Presle, N.; Terlain, B.; Netter, P.; Mainard, D.; Berenbaum, F. Obesity and osteoarthritis: more complex than predicted. *Ann. Rheum. Dis.* **2006**, *65*, 1403–1405.

- (16) Goldring, M. B.; Marcu, K. B. Cartilage homeostasis in health and rheumatic diseases. *Arthritis Res. Ther.* **2009**, *11*, 224.

- (17) Shamoony, M.; Hochberg, M. C. Treatment of osteoarthritis with acetaminophen: efficacy, safety, and comparison with nonsteroidal anti-inflammatory drugs. *Curr Rheumatol Rep* **2000**, *2*, 454–458.

- (18) Alcaraz, M. J.; Megias, J.; Garcia-Arnandis, I.; Clérigues, V.; Guillén, M. I. New molecular targets for the treatment of osteoarthritis. *Biochem. Pharmacol.* **2010**, *80*, 13–21.

- (19) Yan, K.; Shen, Y. Aliskiren has chondroprotective efficacy in a rat model of osteoarthritis through suppression of the local renin-angiotensin system. *Mol. Med. Rep.* **2017**, *16*, 3965–3973.

- (20) Umlauf, D.; Frank, S.; Pap, T.; Bertrand, J. Cartilage biology, pathology, and repair. *Cell. Mol. Life Sci.* **2010**, *67*, 4197–4211.

- (21) Zhu, N.; Hou, J.; Ma, G.; Liu, J. Network Pharmacology Identifies the Mechanisms of Action of Shaoyao Gancao Decoction in the Treatment of Osteoarthritis. *Med. Sci. Monit.* **2019**, *25*, 6051–6073.

- (22) Hopkins, A. L. Network pharmacology. *Nat. Biotechnol.* **2007**, *25*, 1110–1111.

(23) Wu, C. W.; Lu, L.; Liang, S. W.; Chen, C.; Wang, S. M. Application of drug-target prediction technology in network pharmacology of traditional Chinese medicine. *Zhongguo Zhong Yao Za Zhi* **2016**, *41*, 377–382.

(24) Hathout, R. M.; El-Ahmady, S. H.; Metwally, A. A. Curcumin or bisdemethoxycurcumin for nose-to-brain treatment of Alzheimer disease? A bio/chemo-informatics case study. *Nat. Prod. Res.* **2018**, *32*, 2873–2881.

(25) Yang, M.; Chen, J.; Xu, L.; Shi, X.; Zhou, X.; An, R.; Wang, X. A Network Pharmacology Approach to Uncover the Molecular Mechanisms of Herbal Formula Ban-Xia-Xie-Xin-Tang. *Evid Based Complement Alternat Med* **2018**, *2018*, 4050714.

(26) Zhang, L.; Shi, X.; Huang, Z.; Mao, J.; Mei, W.; Ding, L.; Zhang, L.; Xing, R.; Wang, P. Network Pharmacology Approach to Uncover the Mechanism Governing the Effect of Radix Achyranthis Bidentatae on Osteoarthritis. *BMC Complement Med Ther* **2020**, *20*, 121.

(27) Bomer, N.; den Hollander, W.; Ramos, Y. F. M.; Meulenbelt, I. Translating genomics into mechanisms of disease: Osteoarthritis. *Best Pract Res Clin Rheumatol* **2015**, *29*, 683–691.

(28) Carullo, G.; Cappello, A. R.; Frattaruolo, L.; Badolato, M.; Armentano, B.; Aiello, F. Quercetin and derivatives: useful tools in inflammation and pain management. *Future Med. Chem.* **2017**, *9*, 79–93.

(29) Gao, W.; Zan, Y.; Wang, Z. J.; Hu, X. Y.; Huang, F. Quercetin ameliorates paclitaxel-induced neuropathic pain by stabilizing mast cells, and subsequently blocking PKC ϵ -dependent activation of TRPV1. *Acta Pharmacol. Sin.* **2016**, *37*, 1166–1177.

(30) Borghi, S. M.; Pinho-Ribeiro, F. A.; Fattori, V.; Bussmann, A. J. C.; Vignoli, J. A.; Camilios-Neto, D.; Casagrande, R.; Verri, W. A. Quercetin Inhibits Peripheral and Spinal Cord Nociceptive Mechanisms to Reduce Intense Acute Swimming-Induced Muscle Pain in Mice. *PLoS One* **2016**, *11*, No. e0162267.

(31) Britti, D.; Crupi, R.; Impellizzeri, D.; Gugliandolo, E.; Fusco, R.; Schievano, C.; Morittu, V. M.; Evangelista, M.; Di, P. R.; Cuzzocrea, S. A novel composite formulation of palmitoylethanolamide and quercetin decreases inflammation and relieves pain in inflammatory and osteoarthritic pain models. *BMC Vet. Res.* **2017**, *13*, 229.

(32) Petrosino, S.; Di Marzo, V. The pharmacology of palmitoylethanolamide and first data on the therapeutic efficacy of some of its new formulations. *Br. J. Pharmacol.* **2017**, *174*, 1349–1365.

(33) Yang, H.; Li, Y.; Shen, S.; Gan, D.; Han, C.; Wu, J.; Wang, Z. Network Pharmacology-Based Investigation into the Mechanisms of Quyushengxin Formula for the Treatment of Ulcerative Colitis. *Evid Based Complement Alternat Med* **2019**, *2019*, 7870424.

(34) Lee, W. Y.; Lee, C. Y.; Kim, Y. S.; Kim, C. E. The Methodological Trends of Traditional Herbal Medicine Employing Network Pharmacology. *Biomolecules* **2019**, *9*, 362.

(35) Barrett, T.; Troup, D. B.; Wilhite, S. E.; Ledoux, P.; Evangelista, C.; Kim, I. F.; Tomashevsky, M.; Marshall, K. A.; Phillippy, K. H.; Sherman, P. M.; Muerlter, R. N.; Holko, M.; Ayanbule, O.; Yefanov, A.; Soboleva, A. NCBI GEO: archive for functional genomics data sets—10 years on. *Nucleic Acids Res.* **2011**, *39*, D1005–D1010.

(36) Wang, X. P.; Xie, W. P.; Bi, Y. F.; Wang, B. A.; Song, H. B.; Wang, S. L.; Bi, R. X. Quercetin suppresses apoptosis of chondrocytes induced by IL-1 β via inactivation of p38 MAPK signaling pathway. *Exp Ther Med.* **2021**, *21*, 468.